Electronic Supplementary Material (ESI) for New Journal of Chemistry.

Electronic Supplementary Information

Design and synthesis of new functionalized 8-(thiophen-2-yl)-1,2,3,4-tetrahydroquinolines as *turn-off* chemosensors for selective recognition of Pd^{2+} ion

Shally,[a] Vijay Kumar,[a] Ismail Althagafi,[b] Ashish Kumar,[a] Divya Singhal,[a] Abhinav Kumar,[c] Rajiv Gupta[a] and Ramendra Pratap[a]

[a]*Department of Chemistry, University of Delhi, North Campus, Delhi, India, Pin-110007*

[b]*Department of Chemistry, Umm Al-Qura University, Makkah, Saudi Arabia*

[c]*Department of Chemistry, University of Lucknow, Lucknow, Uttar Pradesh, India-226009*

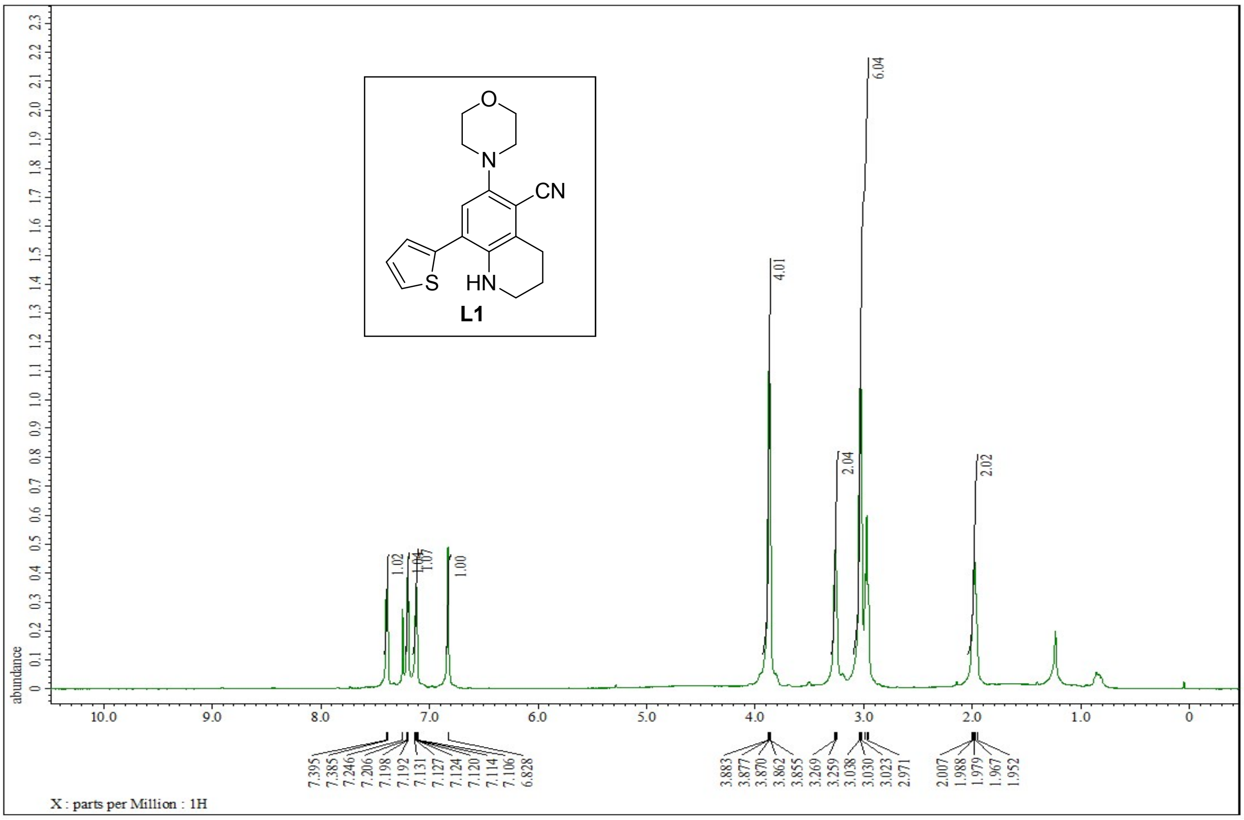

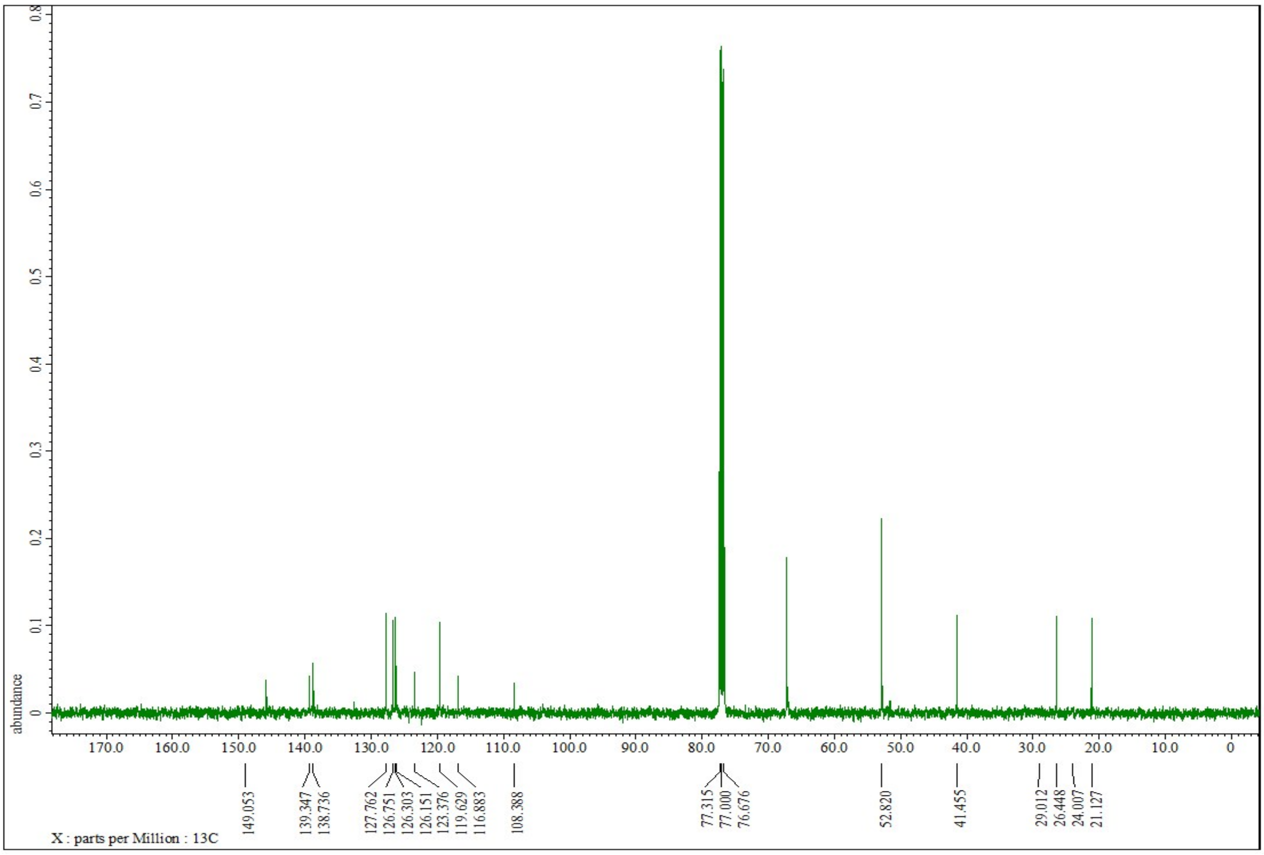

Figure S1: ^{1}H and ^{13}C spectra of L1.

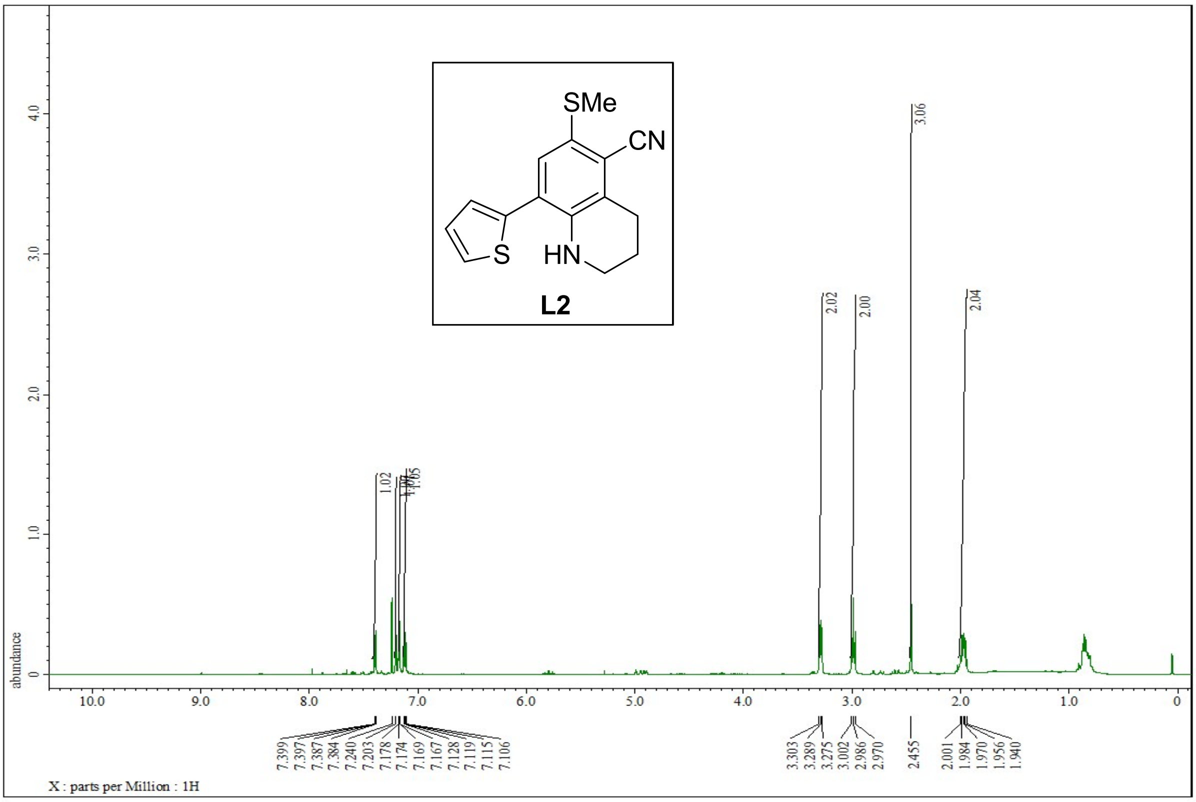

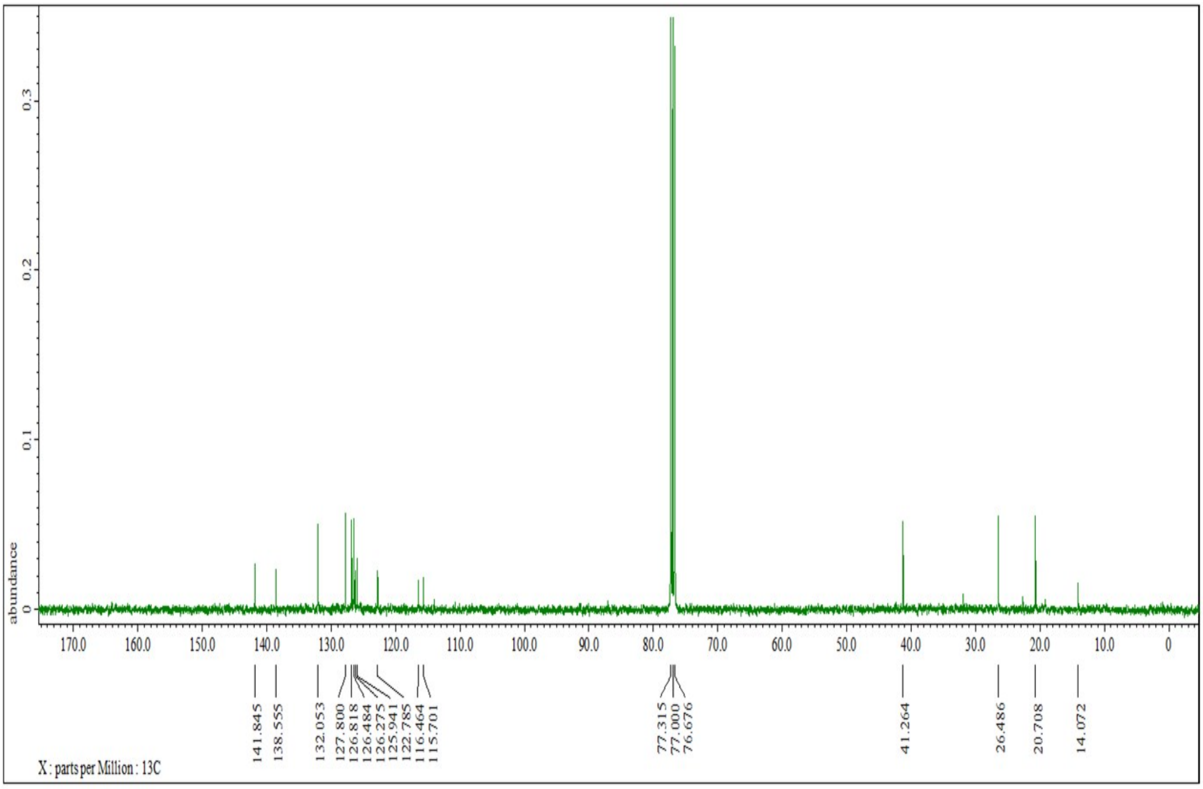

Figure S2: ^{1}H and ^{13}C spectra of L2.

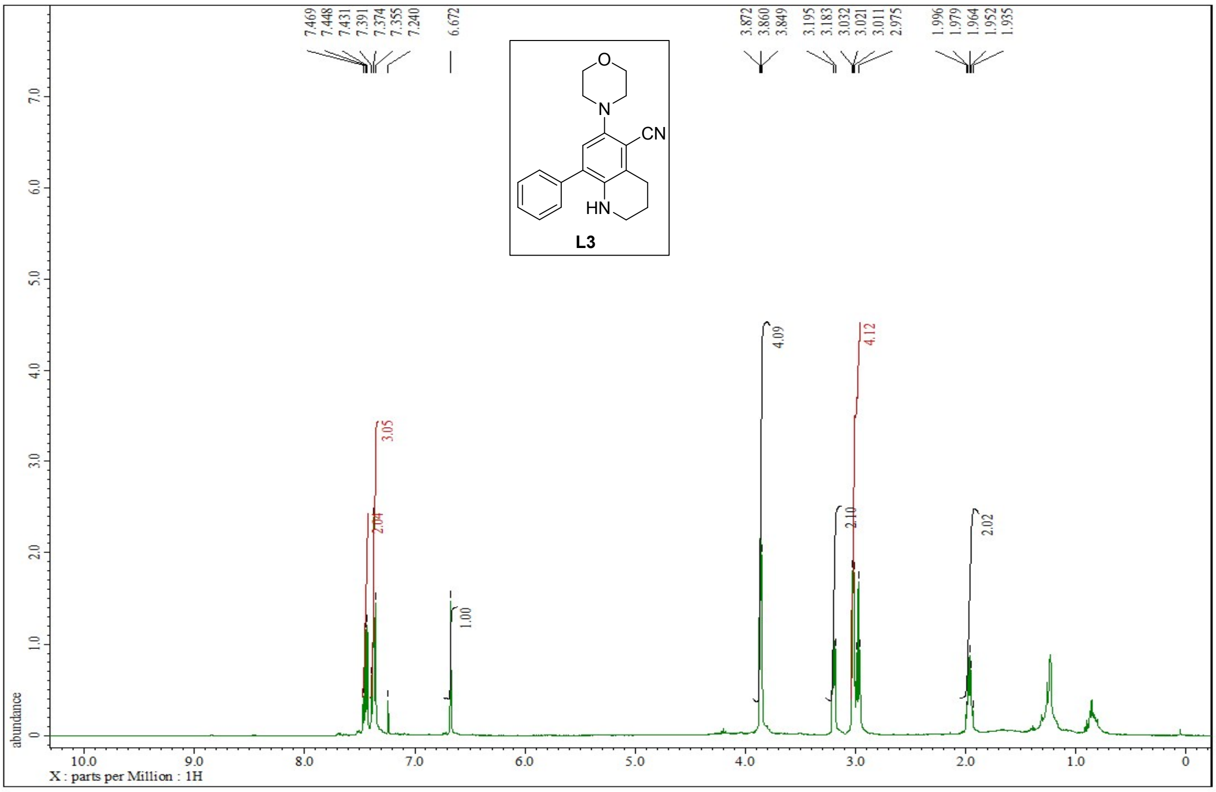

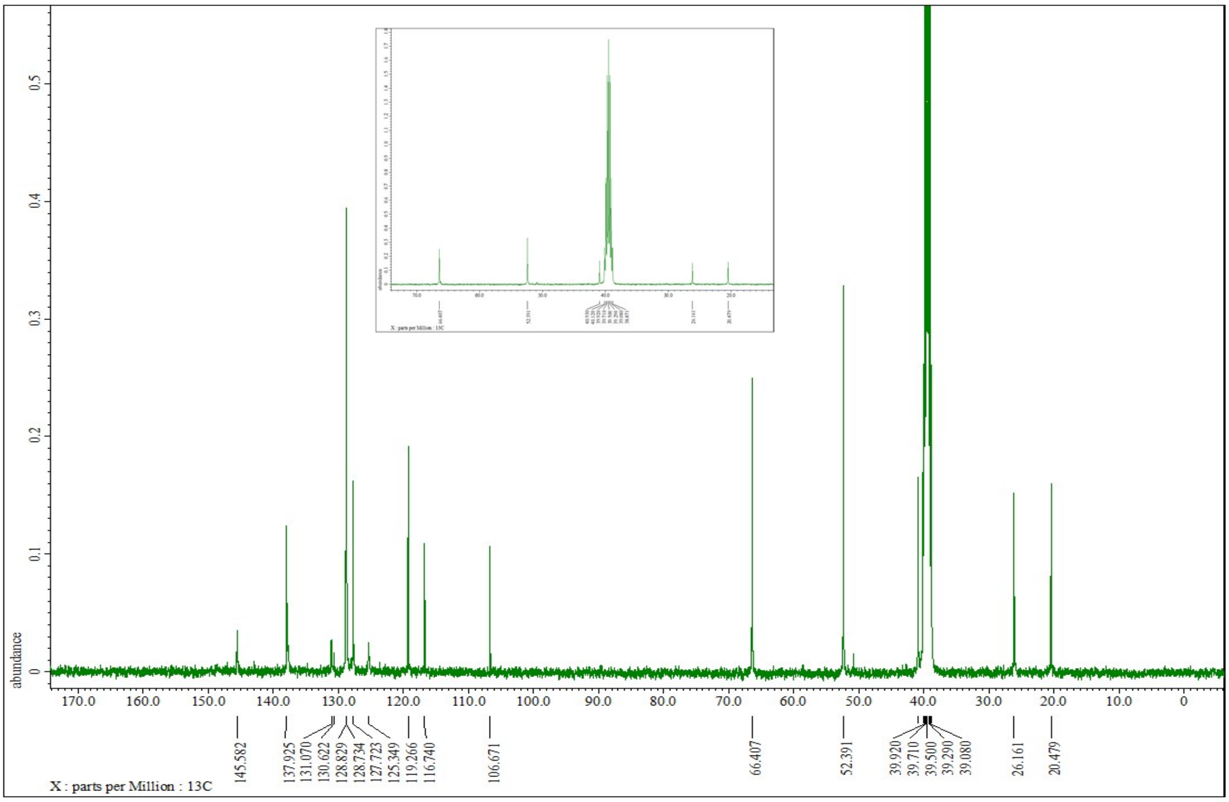

Figure S3: ^{1}H and ^{13}C spectra of L3.

Ligand L1 L-1

Qualitative Compound Report

Data File	SSR -45(D).d	**Sample Name**	SSR -45(D)
Sample Type	Sample	**Position**	P1-D2
Instrument Name	Instrument 1	**User Name**	
Acq Method	29.10.2014.m	**Acquired Time**	22-05-2015 15:39:13
IRM Calibration Status	Success	**DA Method**	Default.m
Comment			

Sample Group		**Info.**
Acquisition SW Version	6200 series TOF/6500 series Q-TOF B.05.01 (B5125)	

Compound Table

Compound Label	RT	Mass	Formula	MFG Formula	MFG Diff (ppm)	DB Formula
Cpd 1: C18 H19 N3 O S	0.196	325.1248	C18 H19 N3 O S	C18 H19 N3 O S	0.25	C18 H19 N3 O S

Compound Label	*m/z*	RT	Algorithm	Mass
Cpd 1: C18 H19 N3 O S	326.1324	0.196	Find by Molecular Feature	325.1248

MFE MS Spectrum

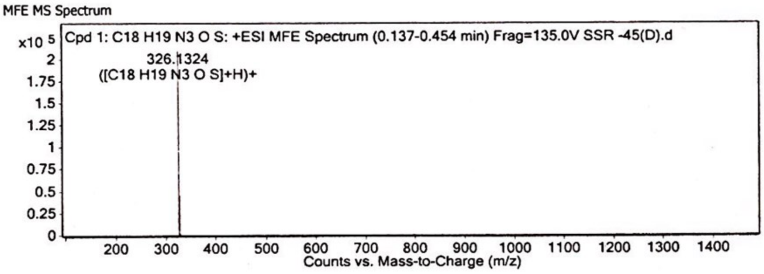

MFE MS Zoomed Spectrum

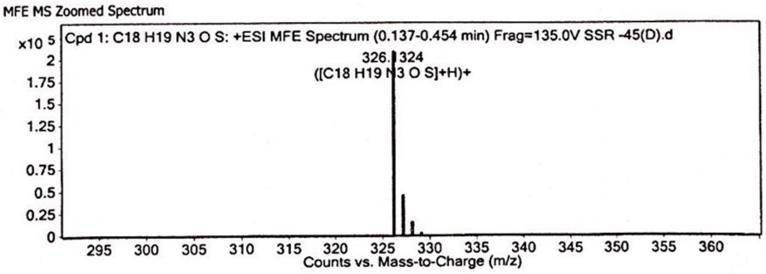

MS Spectrum Peak List

m/z	z	Abund	Formula	Ion
326.1324	1	209244.95	C18 H19 N3 O S	(M+H)+
327.1334	1	45773.17	C18 H19 N3 O S	(M+H)+
328.1316	1	11671.43	C18 H19 N3 O S	(M+H)+
329.1337	1	1811.91	C18 H19 N3 O S	(M+H)+
330.1302	1	146.24	C18 H19 N3 O S	(M+H)+

--- End Of Report ---

Agilent Technologies Page 1 of 1 Printed at: 16:15 on:22-05-2015

Figure S4: HRMS spectra of L1.

Ligand L2

Qualitative Compound Report

L-2

Data File	CSR-320.d	**Sample Name**	CSR-320
Sample Type	Sample	**Position**	P1-C2
Instrument Name	Instrument 1	**User Name**	
Acq Method	29.10.2014.m	**Acquired Time**	15-05-2017 12:58:11
IRM Calibration Status	Success	**DA Method**	Default.m
Comment			

Sample Group		**Info.**
Acquisition SW Version	6200 series TOF/6500 series Q-TOF B.05.01 (B5125)	

Compound Table

Compound Label	RT	Mass	Formula	MFG Formula	MFG Diff (ppm)	DB Formula
Cpd 8: C15 H14 N2 S2	11	286.0595	C15 H14 N2 S2	C15 H14 N2 S2	1.33	C15 H14 N2 S2

Compound Label	*m/z*	RT	Algorithm	Mass
Cpd 8: C15 H14 N2 S2	287.0667	11	Find by Molecular Feature	286.0595

MFE MS Spectrum

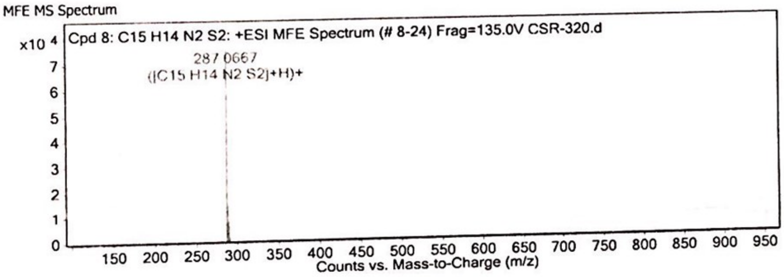

MFE MS Zoomed Spectrum

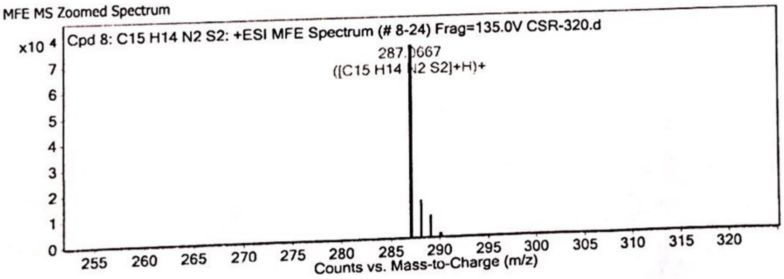

MS Spectrum Peak List

m/z	z	Abund	Formula	Ion
287.0667	1	75639.23	C15 H14 N2 S2	(M+H)+
288.0695	1	14242.25	C15 H14 N2 S2	(M+H)+
289.064	1	7612.32	C15 H14 N2 S2	(M+H)+
290.0666	1	1453.31	C15 H14 N2 S2	(M+H)+

--- End Of Report ---

Figure S5: HRMS spectra of L2.

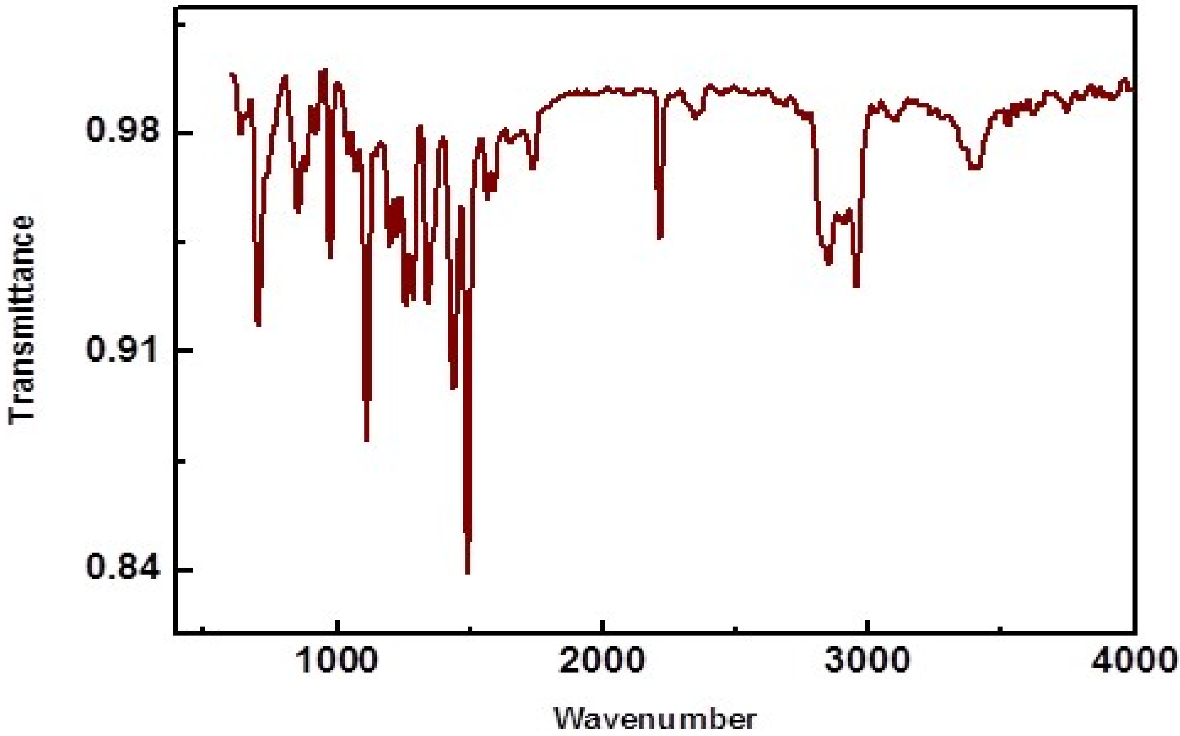

Figure S6: FTIR spectrum of L1.

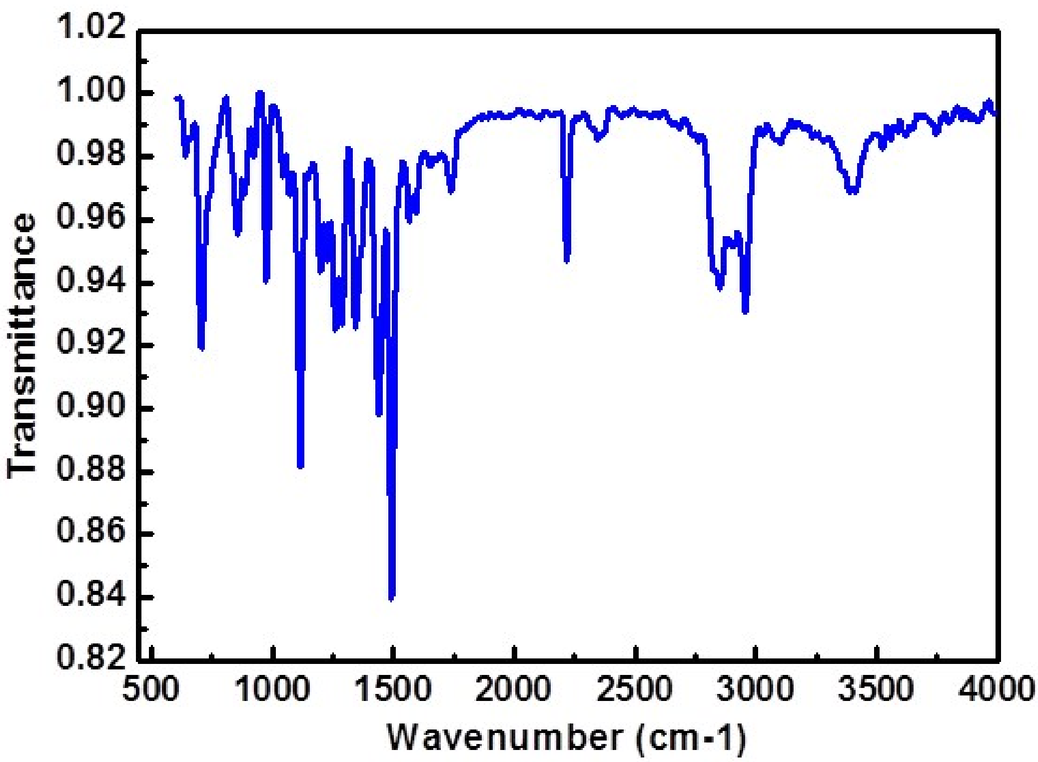

Figure S7: FTIR spectrum of L2.

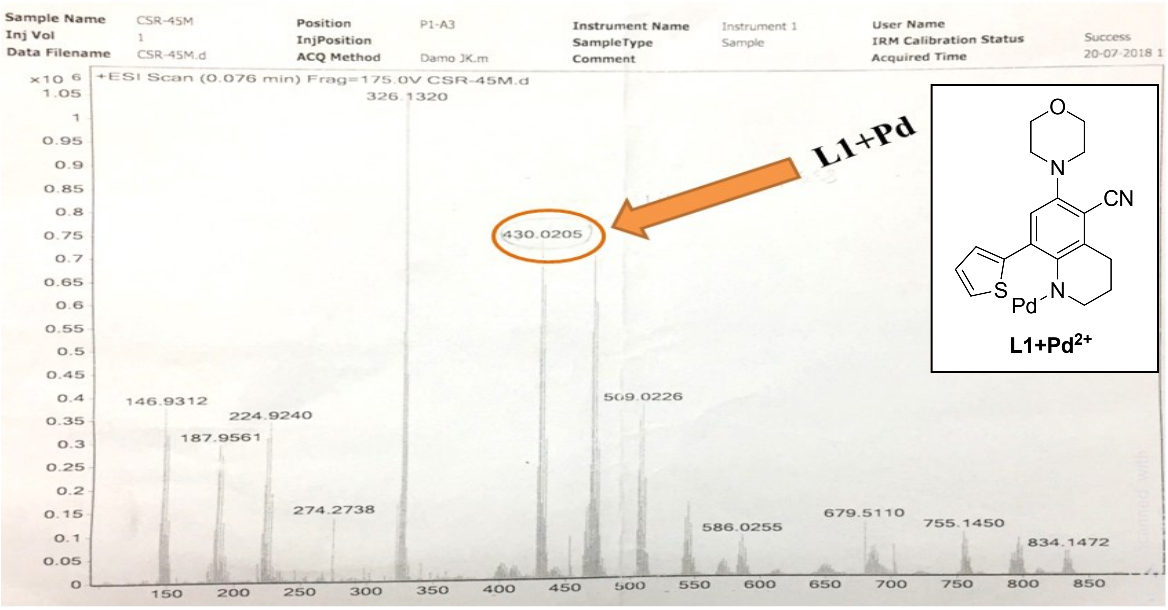

Figure S8: HRMS spectra of L1+Pd^{2+} complex.

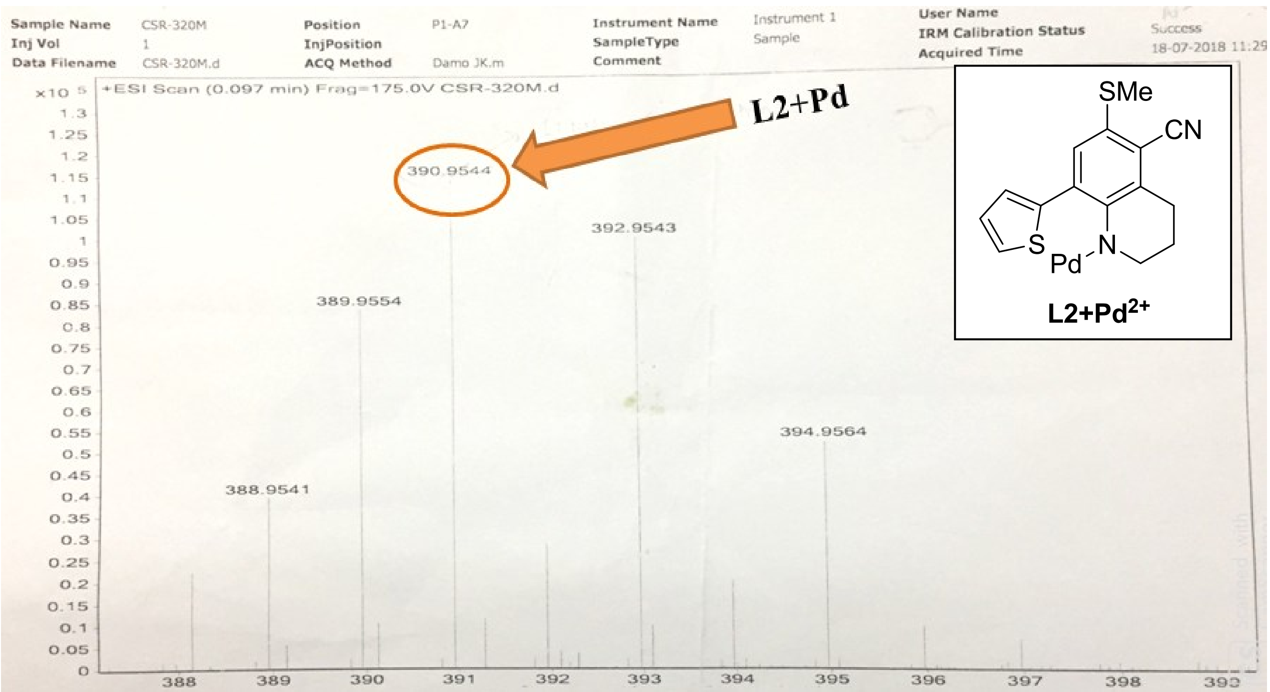

Figure S9: HRMS spectra of L2+Pd^{2+} complex.

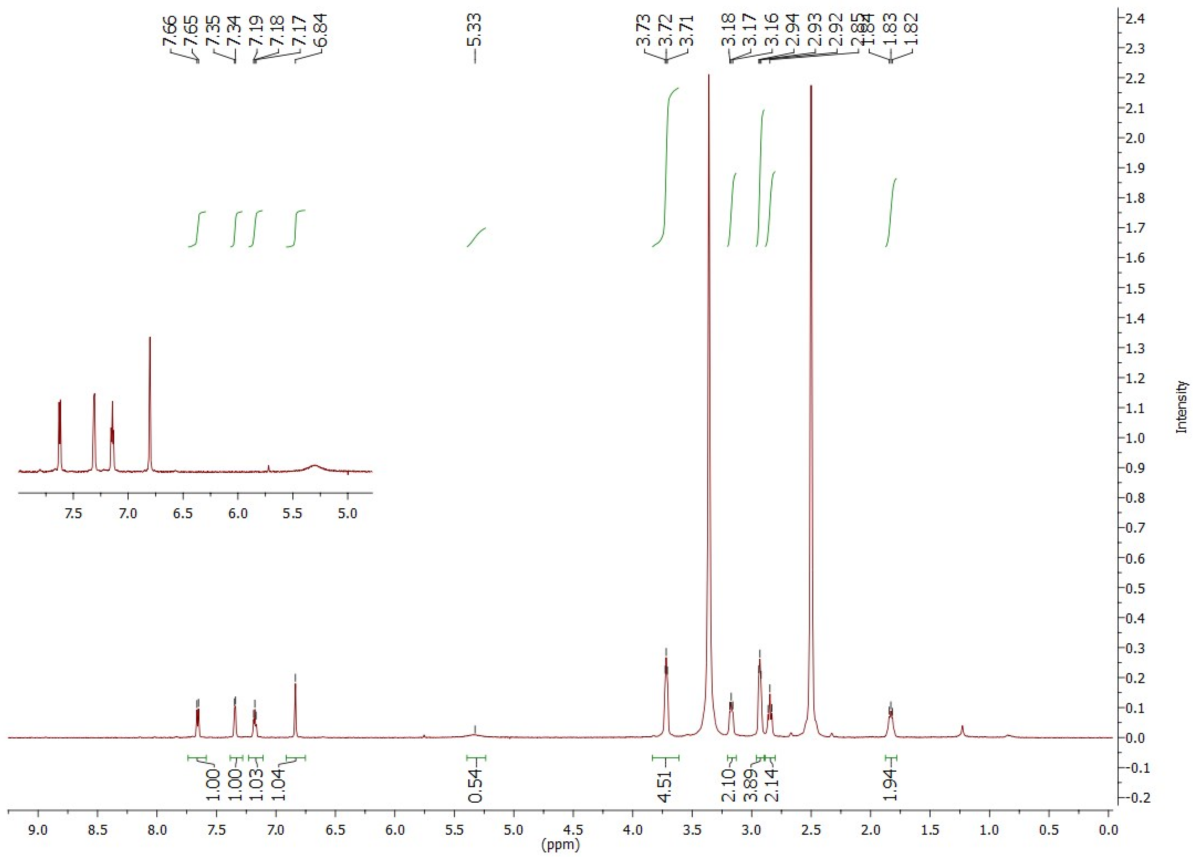

Figure S10: ^{1}H NMR spectra of L1+Pd^{2+} complex with 4.0 equivalent Pd^{2+} ion.

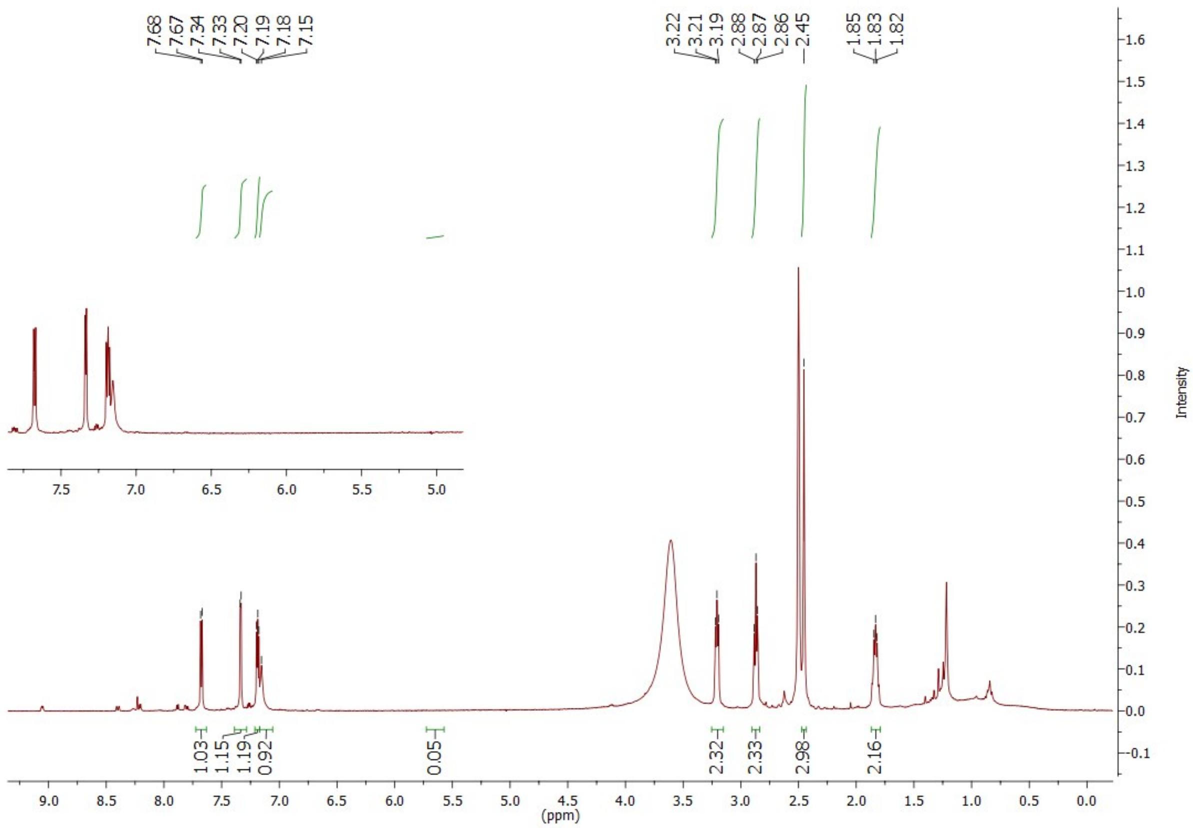

Figure S11: ^{1}H NMR spectra of L2+Pd^{2+} complex with 4.0 equivalent Pd^{2+} ion.

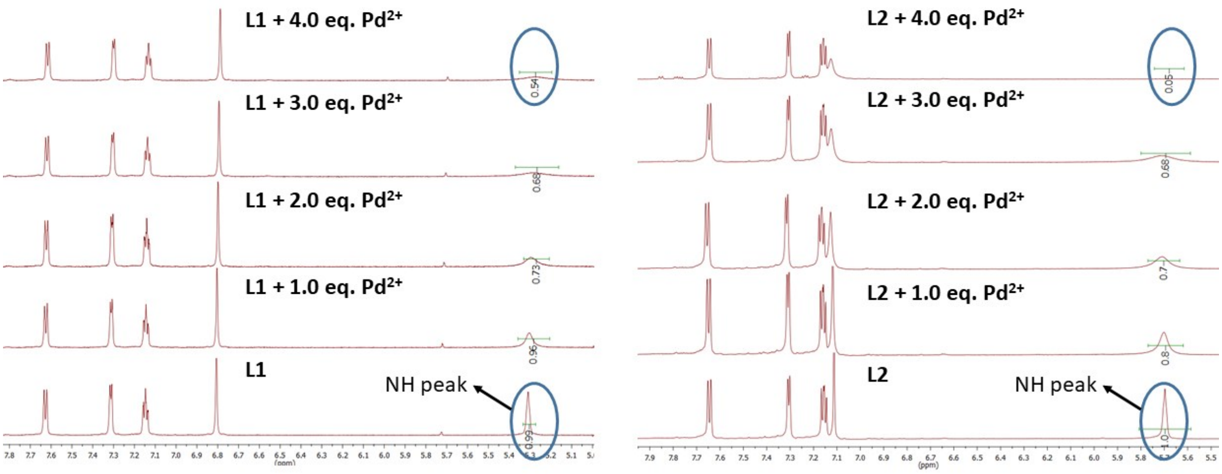

Figure S12: ^{1}H NMR titration of **L1** and **L2** with palladium chloride in DMSO-d_6.

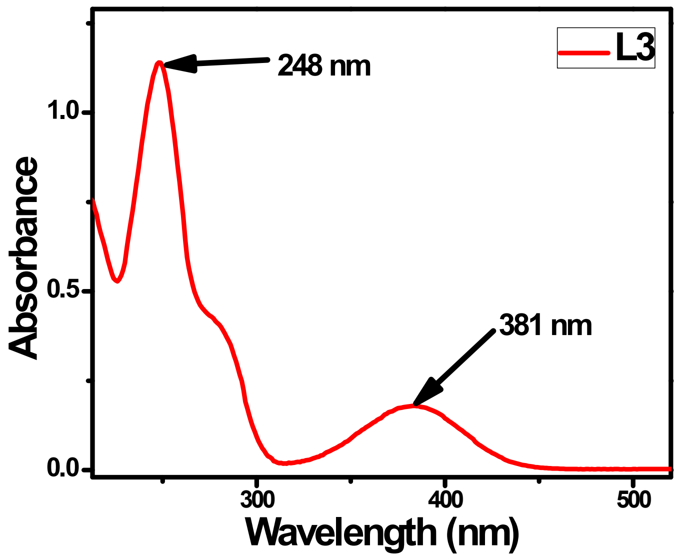

Figure S13: UV-vis spectra of **L3** (20 µM)

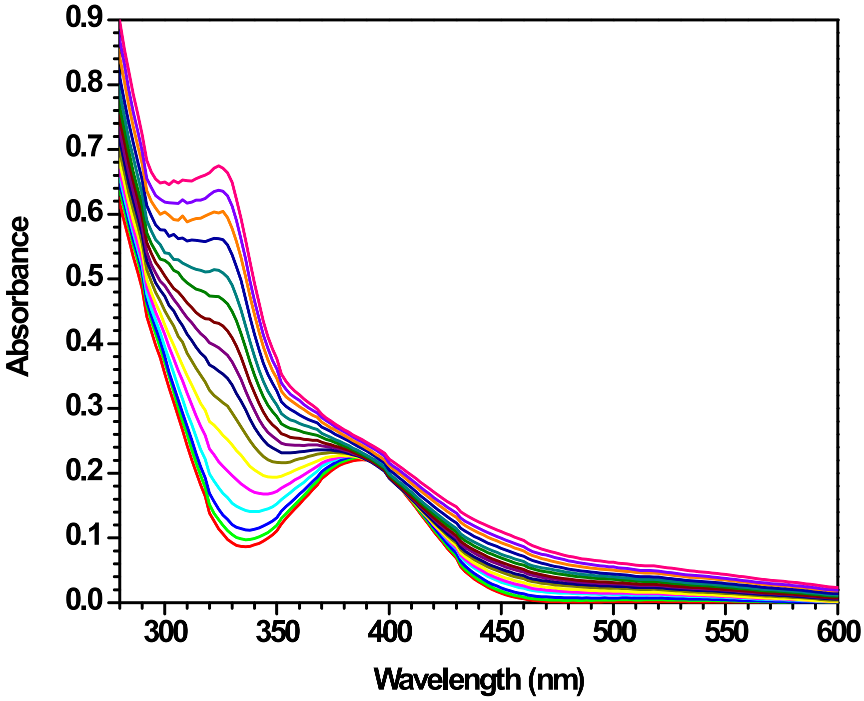

Figure S14: Change in absorption spectra of chemosensor L1 (20 μM) with different concentrations of Pd^{2+} ion (0–50 μM).

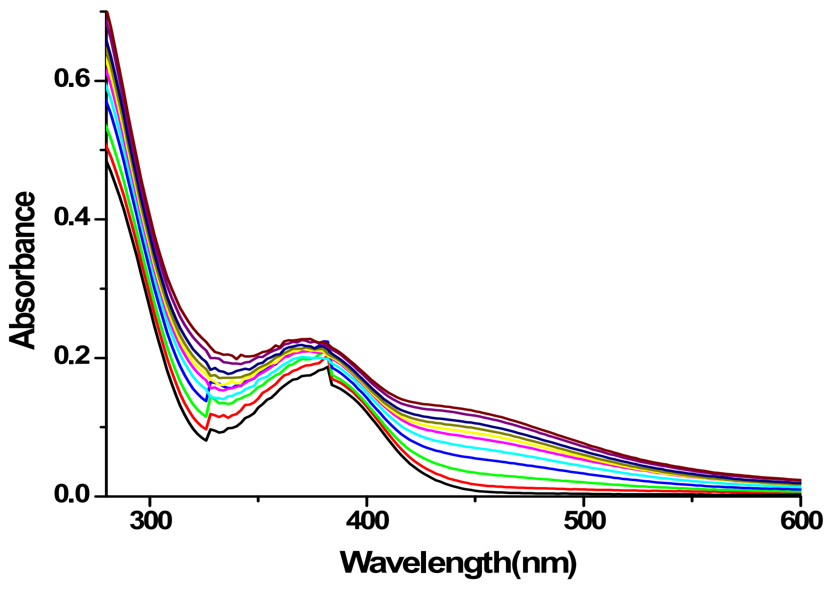

Figure S15: Change in absorption spectra of chemosensor L2 (20 μM) with different concentrations of Pd^{2+} ion (0–50μM).

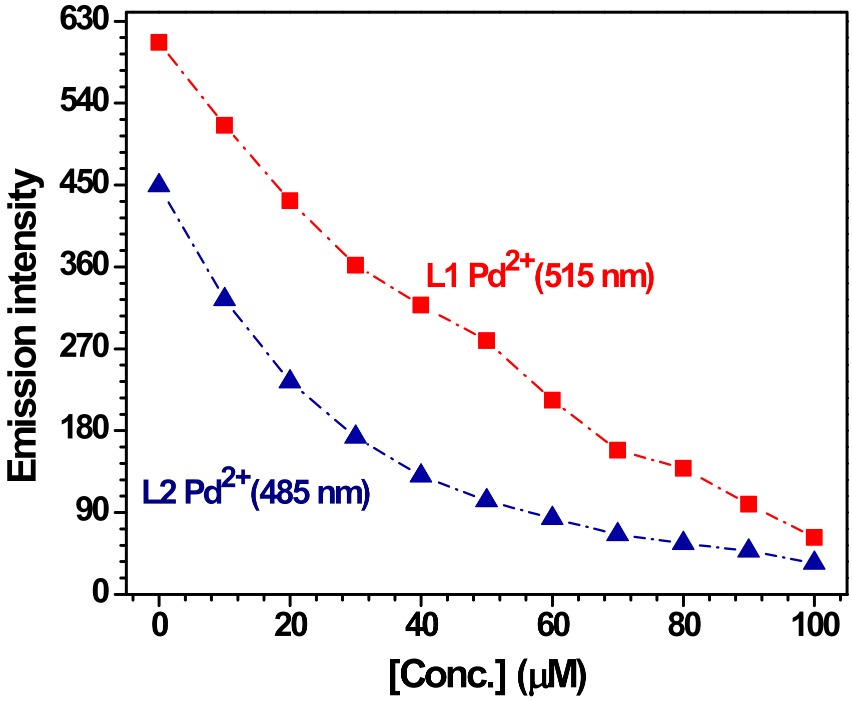

Figure S16: Change in emission intensity of L1 (20 μM) at 515 nm and L2 (20 μM) at 485 nm with varying concentration of Pd^{2+} ions (100 μM).

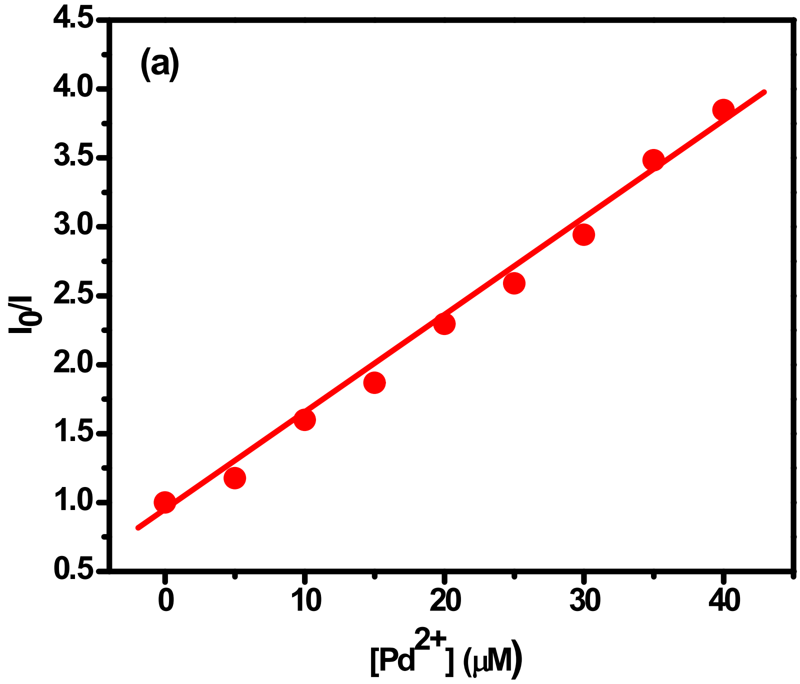

Figure S17: Stern-Volmer plots for the detection of Pd^{2+} ion by chemosensor L1 (50μM).

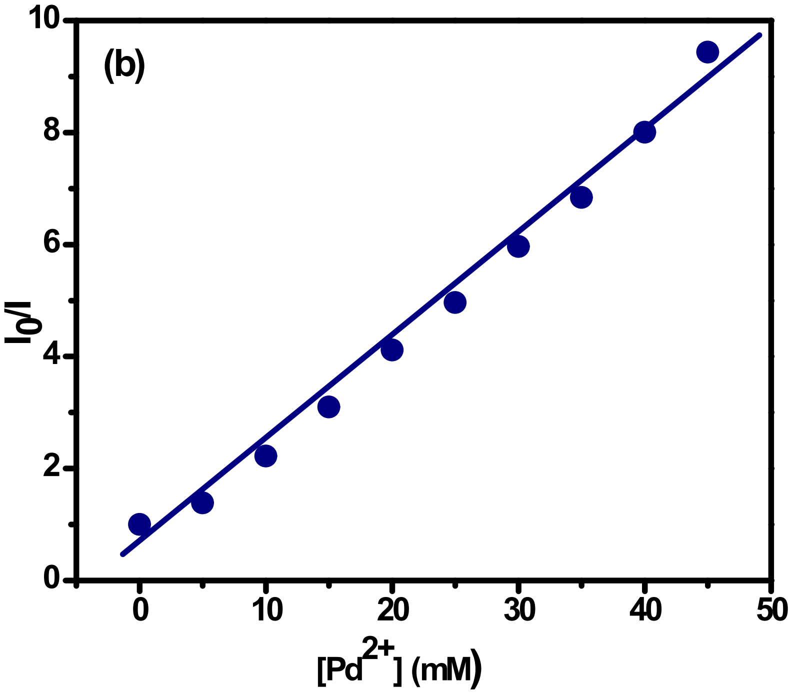

Figure S18: Stern-Volmer plots for the detection of Pd^{2+} ion by chemosensor L2 (50μM).

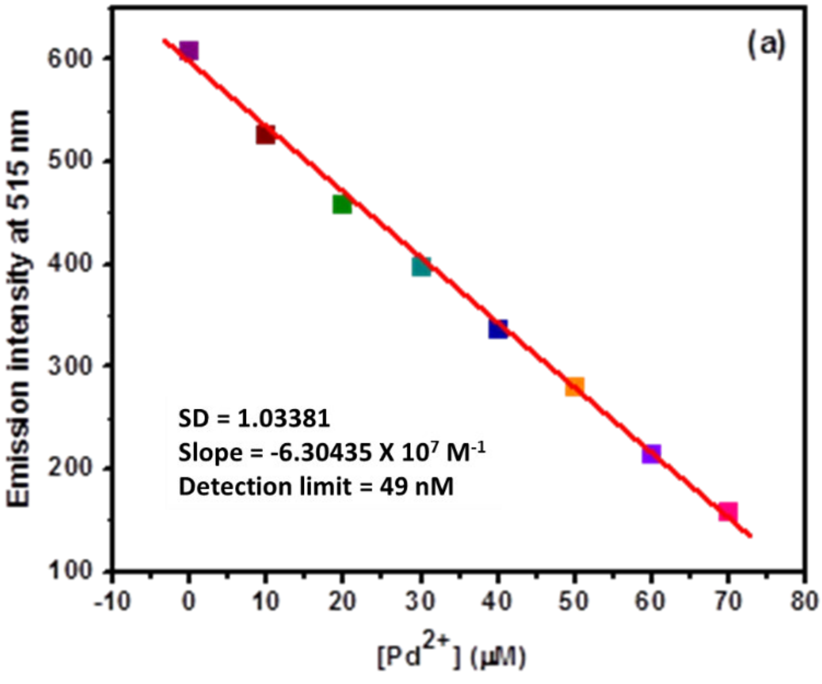

Figure S19: Determination of detection limit of for the detection of Pd^{2+} ion with L1 (20 μM).

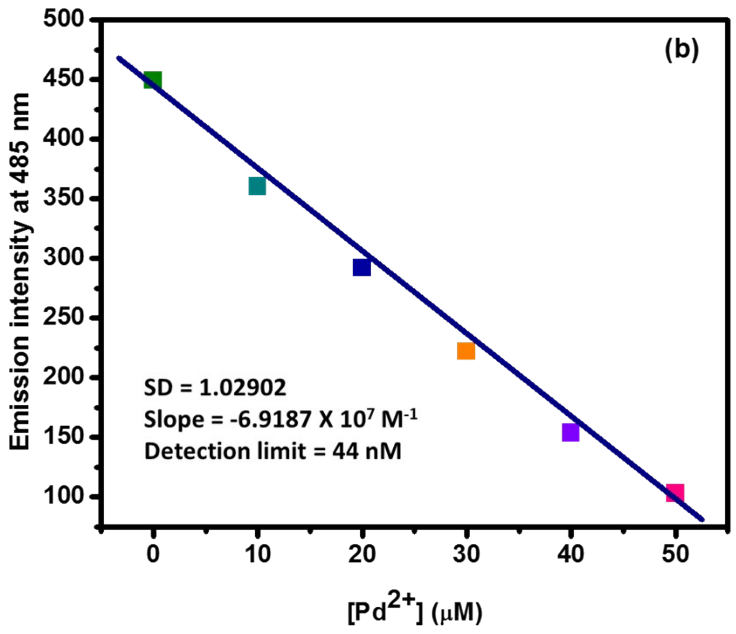

Figure. S20: Determination of detection limit of for the detection of Pd^{2+} ion with L2 (20 μM).

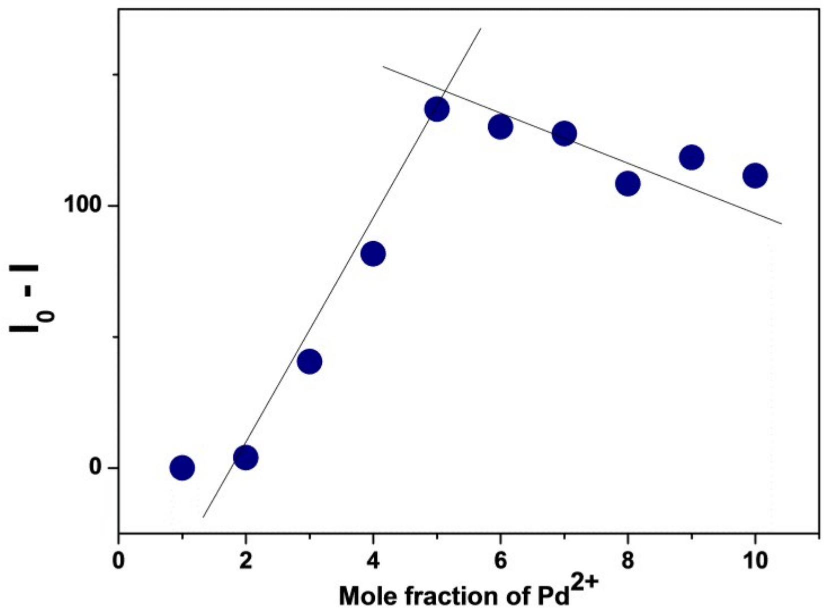

Figure S21: Job's plot for the detection of Pd^{2+} ion by chemosensor L1 in methanol. Total concentrations of chemosensor L1 and Pd^{2+} ion was maintained at 50 μM.

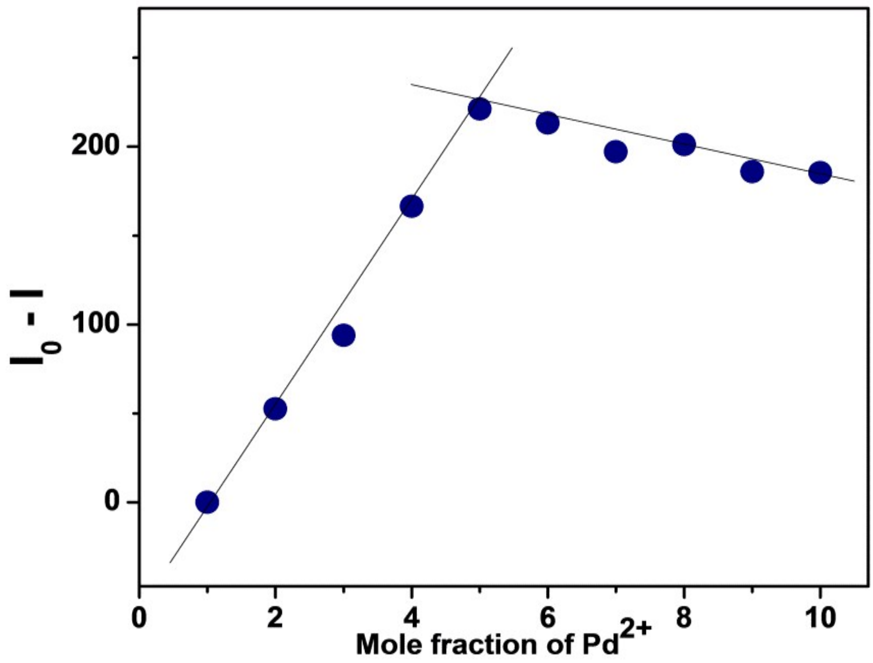

Figure S22: Job's plot for the detection of Pd^{2+} ion by chemosensor L2in methanol. Total concentrations of chemosensor L2 and Pd^{2+} ion was maintained at 50 µM.

Table S1: Lifetime profile of probe L1 and L2 in the absence and presence of Pd^{2+} ion in methanol

L	τ_1 (ns)	τ_2 (ns)	B1	B2	τ_{av}(ns)
L1	1.463	9.631	0.086	0.0501	7.94
L1 + Pd^{2+}	2.543	8.326	0.033	0.078	7.24
L2	0.982	8.075	0.027	0.0951	7.83
L2+Pd^{2+}	2.816	14.343	0.121	0.120	4.74

Table S2 : DFT and HOMO-LUMO band gap of **L1**, **L1 + Pd^{2+}**, **L2** and **L2 + Pd^{2+}**

Energy	**L1**	**L1+Pd^{2+}**	**L2**	**L2+Pd^{2+}**
HOMO (eV)	-8.15	-6.46	-7.94	-6.88
LUMO (eV)	-6.00	-6.00	-6.03	-6.47
Band gap (eV)	2.15	0.46	1.90	0.40

Table S3 : DFT and HOMO-LUMO energy band gap of complex **L1 + Pd^{2}** and **L2 + Pd^{2+}** in presence of H-atom with N-atom of tetrahydroquinoline.

	Optimized structure	**HOMO**	**LUMO**	**Band Gap**
L1	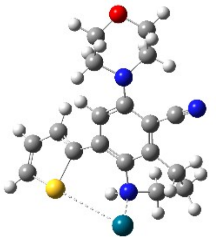	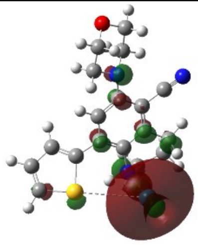	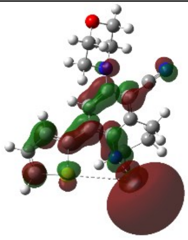	**LUMO** **HOMO**
Energy		**-2.823 eV**	**-0.374 eV**	**2.455 eV**
L2	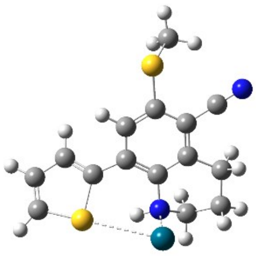	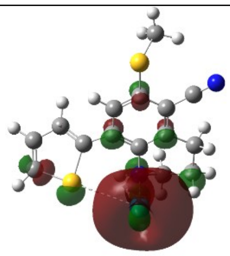	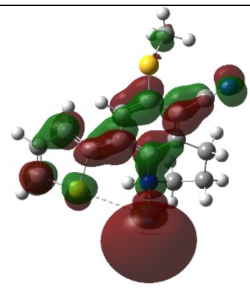	**LUMO** **HOMO**
Energy		**-2.934 eV**	**-0.632 eV**	**2.302 eV**

X-ray Crystallographic Data for compound L1

To a 5 ml glass vial 25-30 mg of 6-morpholino-8-(thiophen-2-yl)-1,2,3,4-tetrahydroquinoline-5-carbonitrile (**L1**) was completely dissolved in DCM followed by addition of 1-2 drops of hexanes. Further, solution was kept for slow evaporation at room temperature until yellow needles type suitable crystal obtained for X-ray analysis.

Crystal data for L1: A yellow crystal (0.220 x 0.200 x 0.180 mm^3) was mounted on a capillary tube for indexing and intensity data collection at 298K on an Oxford Xcalibur Sapphire3 CCD single-crystal diffractometer (MoKα radiation, λ = 0.71073 Å).[1] Routine Lorentz and polarization corrections were applied, and an absorption correction was performed using the ABSCALE 3 program [CrysAlis Pro software system, Version 171.34; Oxford Diffraction Ltd., Oxford, U.K., 2011]. Data reduction was performed with the CrysAllis-PRO.[1] The structure was solved by direct methods using SIR-92 program[2] and refined on F2 using all data by full matrix least-squares procedures with SHELXL-2016/6 incorporated in WINGX 1.8.05 crystallographic collective package.[3] The hydrogen atoms were placed at the calculated positions and included in the last cycles of the refinement. All calculations were done using the WinGX software package.[4-5] Crystallographic data collection and structure solution parameters are summarized in **Table S3**.

Table S4: Crystal data and structure refinement for L1

CCDC No	**1974743**	
Identification code	csr-45	
Empirical formula	C18 H19 N3 O S	
Formula weight	325.42	
Temperature	298(2) K	
Wavelength	0.71073 Å	
Crystal system	Triclinic	
Space group	P -1	
Unit cell dimensions	a = 8.5585(6) Å	a= 83.453(6)°
	b = 8.9403(6) Å	b= 70.241(6)°
	c = 11.5304(7) Å	g = 78.827(6)°
Volume	813.45(9) $Å^3$	
Z	2	
Density (calculated)	1.329 Mg/m^3	
Absorption coefficient	0.207 mm^{-1}	
F(000)	344	
Crystal size	0.220 x 0.200 x 0.180 mm^3	
Theta range for data collection	3.64° to 25.03°	
Index ranges	-10<=h<=10, -10<=k<=10, -13<=l<=13	
Reflections collected	10130	
Independent reflections	2865 [R(int) = 0.0491]	
Completeness to theta = 24.997°	99.6 %	
Refinement method	Full-matrix least-squares on F^2	
Data / restraints / parameters	2865 / 4 / 208	
Goodness-of-fit on F^2	1.055	
Final R indices [I>2sigma(I)]	R1 = 0.0429, wR2 = 0.1126	
R indices (all data)	R1 = 0.0491, wR2 = 0.1179	
Extinction coefficient	n/a	
Largest diff. peak and hole	0.29 and -0.25 $e.Å^{-3}$	

Determination of Stern–Volmer constant (K_{SV}) and detection limit

Fluorescence titrations were further used to calculate the quenching constant with a plot using the Stern–Volmer equation [Eq. 1][6].

$$^{I_0}/_{I} = 1 + K_{SV}[Pd^{2+}] \text{.....................(1)}$$

Where I_0 and I is the emission intensity of molecules in the absence and presence of fluorescence quenching metal ion (Pd^{2+} ion here) respectively. K_{SV} is the Stern–Volmer constant i.e. also called quenching constant. The detection limit was calculated using Eq. 2.[7]

$$LOD = \frac{3\sigma}{k} \text{...................... (2)}$$

Where σ is the standard deviation of blank measurements and k is the slope of a plot of emission intensity with metal ion concentration. Binding stoichiometry of Pd^{2+} complexes determined by Job's plot.[8] The binding constant (K_b) for **L1** and **L2** with Pd^{2+} ion was determined by Benesi–Hildebrand equation (3) with a plot between $1/(I - I_0)$ against $1/[Pd^{2+}]$.[9]

$$^{1}/_{(I - I_0)} = 1/\{K_a(I_0 - I_{min})[Pd^{2+}]\} + {}^{1}/_{(I_0 - I_{min})} \quad \text{................ (3)}$$

Where, I is the emission intensity of L1 and L2 in presence of Pd^{2+} ion at 515 and 485 nm, I_0 is the intensity of L1 and L2 in absence of Pd^{2+} ion and I_{min} is the minimum fluorescence intensity in presence of Pd^{2+} ion. The plot $1/(I - I_0)$ vs. $1/[Pd^{2+}]$ were linear and K_a value was obtained from the slope and intercept of the line.

The relative fluorescence quantum yields were determined with quinine sulfate B ($\Phi_S = 0.54$) in 0.1 M H_2SO_4 as a standard and calculated using the following equation 4.[10]

$$\Phi_X = \Phi_S \times (^{I_X}/_{I_S}) \times (^{A_S}/_{A_X}) \times (^{\eta_X}/_{\eta_S})^2 \quad \text{................ (4)}$$

Where Φ represents quantum yield; A is absorbance at the excitation wavelength; λ_{ex} is the excitation wavelength; η is the refractive index of the solution and subscripts x and s refer to unknown and standard samples respectively. Therefore, the fluorescence quantum yield of ligand and were 0.62 and 0.75 respectively.

Comparison of previously reported Pd^{2+}chemosensors

The chemosensors for Pd^{2+} are summarized in the table and compared his limit of detection, solvents and TLC strip sensing activity with our developed chemosensors (**L1** and **L2**).[11-24] The chemosensor **L1** and **L2** showed best limit of detection (sensitivity) and selectivity than other. The TLC plate sensing was also equated, but most of groups did not reported the sensing with TLC strip. After comparison, we found **L1** and **L2** exhibited best response than listed chemosensors.

Table S5: Comparison of fluorescent probes for Pd^{2+} detection

Compounds	LOD (μM)	Solvents	TLC Plates
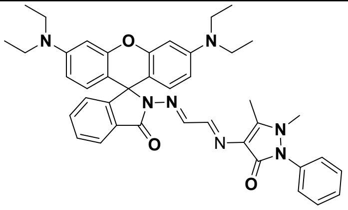	11.9	CH_3CN/H_2O (4:1)	NA
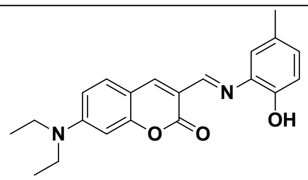	0.74	CH_3CN/ H_2O (4/1, v/v)	Yes
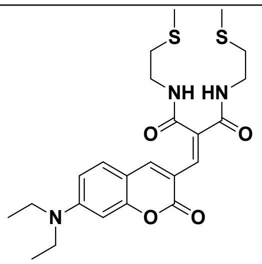	1.0	pH 7.4 HEPES 10 mM, 5% DMSO	NA
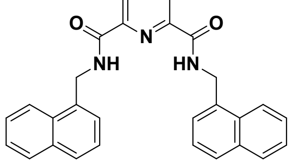 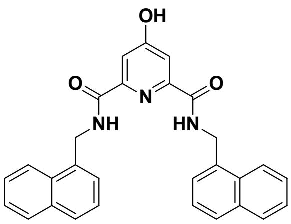	0.78 0.93	HEPES buffer in 1% DMF	Yes
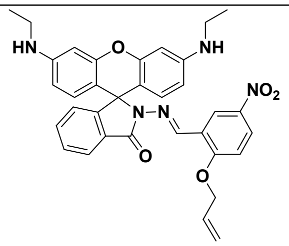	0.095	CH_3CN/H_2O (v/v = 1/4)	NA
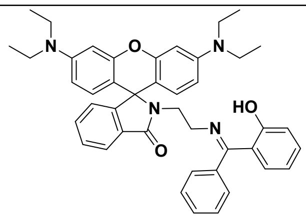	0.034	Aqueous-Ethanolic (v/v, 1:1)	NA

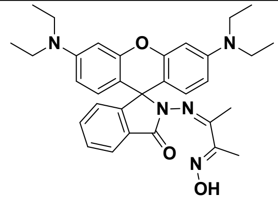	0.200	Tris–HCl buffer	NA
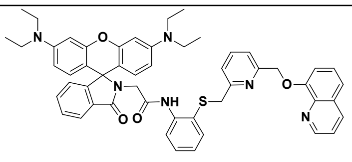 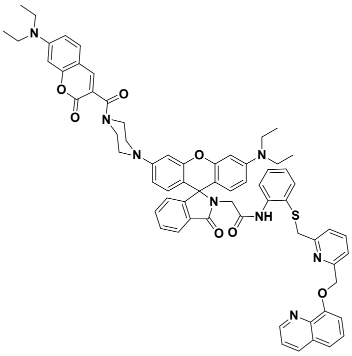	0.070 0.082	Acetonitrile-water (50:50 v/v)	NA
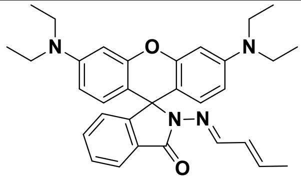	0.19	methanol/PBS (1:1, v/v, pH 7.4)	Yes
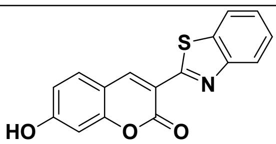	0.29	DMF:H_2O (95:5, v/v)	NA
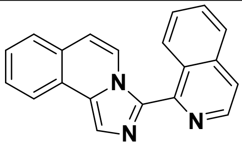	0.210	CH_3OH/aqueous HEPES buffer	Yes
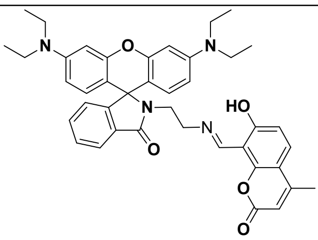	0.18	Ethanol/H_2O (8:2, v/v, HEPES buffer)	NA
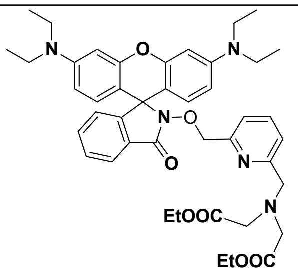	0.25	Aqueous HEPES buffer	NA

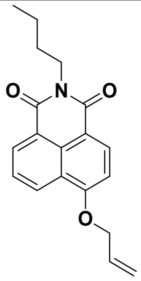	1.4	$Na_2CO_3/NaHCO_3$ buffer solution	NA
Our work 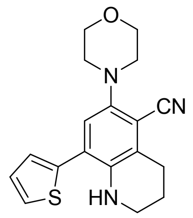 **L1** 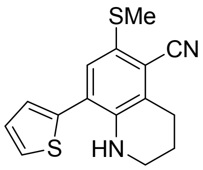 **L2**	**0.049** **0.044**	**MeOH**	**Yes**

References

(1) CrysAlisPro, v. 1.171.33.49b, Oxford Diffraction Ltd., 2009.

(2) A. Altomare, G. Cascarano, C. Giacovazzo and A. Guagliardi, *J. Appl. Cryst*. 1993, **26**, 343.

(3) G. M. Sheldrick, SHELXL-2014/7: Program for the solution of crystal structures, University of Gottingen, Gottingen, Germany, 2014.

(4) G. M. Sheldrick, *Acta Crystallogr., Sect. A:Found. Crystallogr.*, 2008, **64**, 112-122.

(5) L. J. Farrugia, WinGX, v. 1.70, An Integrated System of Windows Programs for the Solution, Refinement and Analysis of Single-Crystal X-ray Diffraction Data, Department of Chemistry, University of Glasgow, 2003.

(6) R. RusakowiczandA. C. Testa, *J. Phys. Chem*. 1968, **72**, 2680–2681.

(7) C. Liang, W. Bu, C. Li, G. Men, M. Deng, Y. Jiangyao, H. Sun and S. Jiang, *Dalton Trans*., 2013, **42**, 1827-1833.

(8) P. Pringsheim, Florescence and Phosphorescence, Interscience Publishing Co., New York, 1949, 333.

(9) A. Senthilvelan, I. Ho, K. Chang, G. Lee, Y. Liu, and W. Chung, *Chem. Eur. J.*, 2009, **15**, 6152–6155.

(10) H. A. Benesi, J. H. A. Hildebrand, *J. Am. Chem. Soc*. 1949, ***71***, 2703–2707.

(11) S. Mondal, S. K. Manna, S. Pathak, A. Al Masum and S. Mukhopadhyaya, *New J. Chem.*, 2019, **43**, 3513-3519

(12) C. K. Manna, S. Gharami, K. Aich, L. Patra and T. K. Mondal, *New J. Chem.*, 2019, **43**, 16915-16920.

(13) M. Lee, T. Lim, Y. Lee, S. Kang and M. S. Han, *Dyes Pigm.,* 2017, **144**, 69-75.

(14) P. Kumar, V. Kumar and R. Gupta, *RSC Adv.,* 2017, **7**, 7734–7741.

(15) A. K. Bhanja, S. Mishra, K. Kar, K. Naskar, S. Maity, K. D. Saha and C. Sinha, *New J. Chem.*, 2018, **42**, 17351-17358.

(16) A. K. Adak, B. Dutta, S. K. Manna, and C. Sinha, *ACS Omega*, 2019, **4**, 18987−18995.

(17) Q. Huang, Y. Zhou, Q. Zhang, E. Wang, Y. Min, H. Qiao, J. Zhang and T. Ma, *Sens. Actuators B: Chem.,* 2015, **208**, 22–29.

(18) F.-K. Tang, S.-M. Chan, T. Wang, C.-S. Kwan, R. Huang, Z. Cai and K. C.-F. Leung, *Talanta* 2020, **210**, 120634.

(19) M. Yang, Y. Bai, W. Meng, Z. Cheng, N. Su and B. Yang, *Inorg. Chem. Commun.,* 2014, **46**, 212-219.

(20) L. Yang, C. Wang, G. Chang and X. Ren, *Sens. Actuators B: Chem.,* 2017, **240**, 212–219.

(21) S. Mahata, A. Bhattacharya, J. P. Kumar, B. B. Mandal and V. Manivannan, *J. Photochem. Photobiol. A: Chem*., 2020, **394**, 112441.

(22) A. K. Adak, R. Purkait, S. Manna, B. C. Ghosh, S. Pathak and C. Sinha, *New J. Chem.*, 2019, **43**, 3899-3906.

(23) M. Li, X.-J. Jiang, H.-H. Wu, H.-L. Lu, H.-Y. Li, H.Xu,S. Q. Zang and T. C. W. Maka, *Dalton Trans*. 2015, **44**, 17326-17334.

(24) X. Li, H. Huang, Y. Zhu, H. Zhao and Z. Wang, *RSC Adv.,* 2015, **5**, 105810-105813.